



Published in final edited form as:

Nat Med. 2010 June ; 16(6): 665–670. doi:10.1038/nm.2143.

ERK activation drives intestinal tumorigenesis in *Apc^{min/+}* mice

Sung Hee Lee^{1,3}, Li-Li Hu¹, Jose Gonzalez-Navajas¹, Geom Seog Seo^{1,4}, Carol Shen¹, Jonathan Brick¹, Scott Herdman¹, Nissi Varki², Maripat Corr¹, Jongdae Lee¹, and Eyal Raz^{1,¶}

¹Department of Medicine, University of California, San Diego La Jolla, CA 92093-0663

²Department of Pathology, University of California, San Diego La Jolla, CA 92093-0663

Abstract

TLR signaling is essential for intestinal tumorigenesis in *Apc^{min/+}* mice, but the mechanisms by which this protein enhances tumor growth are unknown. Here we show that the Microflora-MyD88-ERK signaling in intestinal epithelial cells (IEC) promotes tumorigenesis by increasing the stability of the c-myc oncoprotein. Activation of ERK phosphorylates c-myc that prevents its ubiquitination and its subsequent proteasomal degradation. Accordingly, *Apc^{min/+}/Myd88^{-/-}* mice display reduced levels of pERK and c-myc proteins in IEC, and a low incidence of IEC tumors. A MyD88-independent activation of ERK by EGF increases pERK and c-myc levels and restores the Min phenotype in *Apc^{min/+}/Myd88^{-/-}* mice. Administration of an ERK inhibitor suppressed intestinal tumorigenesis in EGF-treated *Apc^{min/+}/Myd88^{-/-}* and in *Apc^{min/+}* mice and increased their survival. Our data reveal a new facet of oncogene-environment interaction, where the microflora-induced TLR activation regulates the expression of an oncogene that leads to IEC tumor growth in a susceptible host.

Introduction

The gastro-intestinal tract is constantly exposed to a vast number of commensal bacteria and their inflammatory products. Essential to intestinal homeostasis are pattern recognition receptors (PRR) such as TLR¹. Engagement of TLR with their cognate ligands in the intestinal mucosa provokes the production of pro-inflammatory, pro-angiogenic and growth factors that support IEC differentiation and proliferation². In a genetically susceptible host, an on-going intestinal inflammation provokes an uncontrolled growth of IEC leading to neoplasia^{3,4,5}. Likewise, it was proposed that signaling through TLR regulates IEC tumor development, in mice heterozygous for a mutant form of the tumor suppressor gene,

Users may view, print, copy, download and text and data- mine the content in such documents, for the purposes of academic research, subject always to the full Conditions of use: http://www.nature.com/authors/editorial_policies/license.html#terms

[¶] To whom correspondence should be addressed.

³Current address: College of Pharmacy, Wonkwang University, Iksan, Chonbuk 570-749, Republic of Korea

⁴Current address: Wonkwang University School of Medicine, Iksan, Chonbuk 570-749, Republic of Korea

The authors declare that they have no competing financial interest.

Author contributions. E.R. designed the study, S.H.L. and J.L. performed the signaling experiments, C.S., L.H., S.H. and G.S.S. performed the *in vivo* studies, M.C. generated the bone marrow chimeras, J.B., J.L. and J.G. performed immunohistochemistry and flow cytometry, S.H.L., M.P.C, N.V., J.L. and E.R. analyzed the data, and S.H.L., J.L. and E.R. wrote the manuscript.

adenomatous polyposis coli (*Apc*)⁶. However, the molecular mechanisms and its relationship to intestinal inflammation have not been identified. The *Apc*^{min/+} mouse is an animal model of human familial adenomatous polyposis⁷. These mice develop multiple intestinal neoplasia (Min), after they lose the heterozygote wild type *Apc* allele and consequently die when they reach 6 months of age⁸.

The survival and growth of certain tumors are dependent on the continued activation of certain oncogenes. This phenomenon that was termed “oncogene addiction”, explains tumor suppression due to the inactivation of a single gene product⁹. The oncogene *c-myc* is critical for *Apc*-mediated tumorigenesis^{10,11}. The genetic deletion of *c-myc* results in the inhibition of tumor growth¹¹ and as low as a two-fold reduction in *c-myc* expression in IEC is sufficient to inhibit tumorigenesis in *Apc*^{min/+} mice¹²⁻¹⁴. Here we identified that a MyD88-dependent activation of ERK in IEC is essential to drive intestinal tumor growth in *Apc*^{min/+} mice. Consequently, the inhibition of pERK abrogates the Min phenotype in these animals.

Results

MyD88 signaling is essential for polyp growth in *Apc*^{min/+} mice

TLRs signal mainly through either MyD88 or TRIF. To explore the potential impact of TLR signaling on IEC tumors we crossed *Apc*^{min/+} mice to *Myd88*^{-/-} or *Trif*^{Lps2/Lps2} (*Lps2*) mice¹⁵. The average survival was 23 weeks for *Apc*^{min/+} mice and 28 weeks for *Apc*^{min/+}/*Lps2* mice. In contrast, all of the *Apc*^{min/+}/*Myd88*^{-/-} mice survived the 45-week study (Supp. Fig. 1A). We then determined the role of each adapter protein on tumor (polyp) formation at 20 weeks of age. *Apc*^{min/+}/*Myd88*^{-/-} mice had fewer polyps throughout the small and large intestines compared to *Apc*^{min/+} or *Apc*^{min/+}/*Lps2* mice (Supp. Fig. 1B and Supp. Fig. 1C), but they displayed circular raised lesions (microadenomas) in both the distal small intestine (DSI) and the colon (Supp. Fig. 1C-1F).

MyD88 signaling enhances IEC proliferation and suppresses IEC apoptosis in *Apc*^{min/+} mice

As the polyps in the *Apc*^{min/+}/*Myd88*^{-/-} mice failed to grow (Supp. Fig. 1C), we investigated whether the deletion of *Myd88* affected IEC proliferation. The proliferation and the migration rate of IEC along the crypt-villus axis, as analyzed by BrdU incorporation, were decreased as compared to those in *Apc*^{min/+} mice (Fig. 1A). We also observed a significantly higher number of apoptotic IEC in *Apc*^{min/+}/*Myd88*^{-/-} (Fig. 1B) as well as increased levels of cleaved poly(ADP-ribose) polymerase (PARP), a substrate of caspase-3¹⁶ (Fig. 1C). Taken together, these data indicate that TLR signaling via MyD88 enhances IEC proliferation and inhibits IEC apoptosis, and suggest that these two effects synergize in enhancing IEC tumor growth in the *Apc*^{min/+} mice.

Myd88 signaling in IEC, but not in hematopoietic cells, controls IEC tumor growth in *Apc*^{min/+} mice

In the intestinal mucosa, both IEC and bone marrow (BM)-derived cells have functional TLR that utilize MyD88 for signaling^{17,18,19}. To further identify the role of BM-derived cells in IEC tumorigenesis, we generated BM chimeras: both *Apc*^{min/+} and *Apc*^{min/+}/*Myd88*^{-/-}

recipients were reconstituted with BM harvested from either WT or *Myd88*^{-/-} donors²⁰. Reconstitution of *Apc*^{min/+} recipients with either *Myd88*^{-/-} or WT BM did not significantly alter polyp count and growth in either the DSI or the colon. Similarly, the number of polyps did not significantly change in *Apc*^{min/+}/*Myd88*^{-/-} recipients reconstituted with WT or *Myd88*^{-/-} BM (Fig. 2A). These results indicate that polyp growth in *Apc*^{min/+} mice does not depend on TLR-MyD88 signaling in BM-derived cells and highly suggests its dependence on TLR-MyD88 activation of IEC.

To explore whether host-derived or microbial-derived TLR ligands play a role in IEC tumorigenesis, we crossed *Apc*^{min/+} mice with *Il1r1*^{-/-} or with *Caspase1*^{-/-} mice, which are limited in processing IL-1 and IL-18²¹. As presented in Fig. 2B, there was no significant difference in the numbers of polyps in *Apc*^{min/+}/*Il1r1*^{-/-} or *Apc*^{min/+}/*Caspase1*^{-/-} as compared to *Apc*^{min/+} mice. In addition, administration of the IL-1R antagonist, Anakinra, did not affect the extent of IEC tumorigenesis in *Apc*^{min/+} mice (Fig. 2C). Collectively, these data strongly suggest that MyD88-dependent TLR activation by microbial ligands is responsible for IEC tumor growth in *Apc*^{min/+} mice.

A MyD88-dependent TLR signaling upregulates c-myc in IEC

The decrease in IEC proliferation and the increase in IEC apoptosis in *Apc*^{min/+}/*Myd88*^{-/-} mice suggested the involvement of a MyD88-dependent oncogene or mitogen in IEC tumorigenesis. Since c-myc is essential for tumorigenesis in *Apc*^{min/+} mice^{11,12,14}, we tested whether MyD88 regulates the expression of c-myc. MyD88-deficiency resulted in a significant decrease in the c-myc protein level in IEC. While c-myc was expressed throughout the crypt in both the DSI and the colon of *Apc*^{min/+} mice, its expression in *Apc*^{min/+}/*Myd88*^{-/-} mice was restricted to the base of the crypt (Fig. 3A). Immunoblotting analysis of c-myc in isolated IEC (DSI) confirmed the reduced expression of not only c-myc, but also pERK in *Apc*^{min/+}/*Myd88*^{-/-} mice (Fig. 3B and Supp. Fig. 2A). The decreased c-myc level in *Apc*^{min/+}/*Myd88*^{-/-} IEC was observed in both normal and tumor regions (Supp. Fig. 2B). However, the c-myc mRNA levels in IEC did not differ significantly between *Apc*^{min/+} and *Apc*^{min/+}/*Myd88*^{-/-} mice (Fig. 3C). Inactivation of *Apc* activates β-catenin, which induces transcription of c-myc. The deletion of *Myd88* did not affect the β-catenin level *in vivo* (Fig. 3B) or Wnt3-induced activation of β-catenin *in vitro* (Fig. 3D). Collectively, these data indicate that MyD88 signaling affects tumorigenesis independently of the Wnt-APC-β-catenin pathway.

A posttranslational modification of c-myc by TLR-MyD88-ERK pathway stabilizes c-myc expression

The data suggested that MyD88-mediated signaling in IEC provokes tumor growth. Since IEC express functional TLRs^{18,19} and Supp. Fig. 3A, we tested whether activation of a TLR-MyD88 pathway directly induces c-myc. Indeed, activation of TLR2 enhanced the protein level of c-myc in an IEC line RKO (*Apc* wild type) (Fig. 4A) in a MyD88-dependent manner (Supp. Fig. 3B). TLR5 (a MyD88-dependent TLR) activation in RKO produced a similar result (Supp. Fig. 3C). Consistent with the results obtained *in vivo* (Fig. 3C), the level of c-myc mRNA was not affected by TLR2 triggering, while the levels of IL-8 and IκBα were increased¹⁹ (Fig. 4A).

The increase in c-myc protein level without a concomitant increase in mRNA level upon TLR stimulation, suggested that c-myc protein is subjected to post-translational modifications²². Indeed, inhibition of proteasomal function by MG-132 enhanced the c-myc protein levels in RKO cells without affecting the mRNA level (Fig. 4B), indicating a steady state degradation of c-myc. We therefore tested whether TLR stimulation in IEC stabilizes c-myc protein. While the c-myc-ubiquitin conjugates were easily detected even in the absence of a proteasome inhibitor in RKO cells, they rapidly disappeared upon TLR2 stimulation with a concomitant increase in unconjugated c-myc protein (Fig. 4C). These data indicate that the TLR-MyD88-mediated signaling pathway stabilizes c-myc protein in IEC by inhibiting its proteasomal degradation.

MEK/ERK pathway phosphorylates c-myc on Serine 62, which stabilizes c-myc by preventing ubiquitin/proteasomal degradation^{23,24,25}. We examined whether Myd88-mediated activation of ERK is responsible for the stabilization of c-myc. Indeed TLR2 activation induced the phosphorylation of ERK as well as of c-myc on Serine 62 (Fig. 4A). In addition, blocking ERK activation with pharmacological inhibitors rapidly reduced c-myc level (Fig. 4D). Caco-2, another IEC line, expresses a truncated APC protein similar to that observed in *Apc^{min/+}* mice²⁶. We therefore tested whether MyD88-dependent ERK activation can stabilize c-myc in these *Apc* mutant cells. Indeed, TLR2 stimulation increased the c-myc protein level with concomitant ERK activation and a decrease in the polyubiquitinated c-myc (Supp. Fig. 4A and B). Similarly, stimulation of either TLR2 or EGFR in a non-transformed IEC line derived from the small intestine (RIE-1) also activated ERK and c-myc (Supp. Fig. 4C). These data indicate that c-myc level in *Apc^{min/+}* mice is maintained by two independent mechanisms, 1) a transcriptional activation of c-myc by β -catenin signaling initiated by *Apc* inactivation and 2) a post-translational stabilization of c-myc by MyD88-dependent ERK activation.

ERK signaling drives the Min phenotype

We tested whether a MyD88-independent activation of ERK increases c-myc protein level in *Apc^{min/+}/Myd88^{-/-}* mice and restores the Min phenotype. As EGF activates ERK and enhances c-myc levels in non-transformed IEC (Supp. Fig. 4C), we treated *Apc^{min/+}/Myd88^{-/-}* mice with either EGF alone or with EGF plus a MEK1/2 inhibitor (PD0325901, PD). The latter is a specific and an effective pharmacological inhibitor of ERK²⁷ and is in phase II clinical trials. The administration of EGF significantly increased the number of polyps in the DSI (for comparison see Supp. Fig. 1B), and this induction was abrogated by PD treatment (Fig. 5A). Serum hemoglobin and body weights drop significantly in *Apc^{min/+}* mice over time, due to the increase in numbers and the sizes of the exophytic polypoid intestinal tumors minimizing food absorption, with subsequent intestinal obstruction and intestinal bleeding²⁸. The inhibition of tumor growth in *Apc^{min/+}/Myd88^{-/-}*, PD-treated animals coincided with increased serum hemoglobin levels (Fig. 5B) and increased body weight (Fig. 5C), indicating that these were healthier animals. As expected, EGF administration enhanced levels of c-myc and pERK in IEC, which was reversed by PD treatment (Fig. 5D). Taken together, the inhibition of IEC tumors in PD treated mice further validated the regulatory role of ERK on tumorigenesis in *Apc^{min/+}/Myd88^{-/-}* mice (Fig. 3B)

and could suggest that TLR-MyD88 pathway contributes significantly to ERK activation in *Apc^{min/+}* mice, under the steady state conditions.

These results indicated a pivotal role for ERK activation in the Min phenotype. We therefore tested its tumorigenic role in 10-week old *Apc^{min/+}* mice. PD treatment for 14 weeks of these animals resulted in complete inhibition of polyp growth (Fig. 6A) with the concomitant increase in serum hemoglobin levels (Fig. 6B) and body weight (Fig. 6C). PD treatment inhibited the levels of both c-myc and pERK in IEC of these mice (Fig. 6D and 6E). Furthermore, PD treatment resulted in 100% survival whereas treatment of control animals with vehicle resulted in 100% mortality during the 17 weeks treatment period of *Apc^{min/+}* mice (Fig. 6F). To detect the long-term effects of PD treatment, we delivered it or vehicle to already 17-week PD-treated *Apc^{min/+}* mice, for additional 15 weeks. Continuous PD treatment inhibited tumorigenesis while its discontinuation provoked high tumor count (Fig. 6G). Collectively, these results indicate that the regulation of ERK pathway in *Apc^{min/+}* mice controls intestinal tumorigenesis and the subsequent manifestation of the Min phenotype, most likely via post-translational modifications of c-myc protein.

Discussion

Overt inflammation can promote neoplasia^{29,30,31,32}. TLR activation of innate immune cells (e.g., macrophages) in the intestinal mucosa provokes the production of various pro-inflammatory mediators^{3,5}. This mechanism was proposed to enhance tumorigenesis in the *Apc^{min/+}* mice⁶. However, our study indicates that MyD88 in non-hematopoietic cells, such as IEC, is required for intestinal tumor growth in the *Apc^{min/+}* mouse. Furthermore, we identified that TLR ligands presumably from intestinal flora (Fig. 4), and not from the host (Fig. 2), mediate IEC tumor growth under the steady-state conditions. In this setting, MyD88-mediated signaling, induces ERK activation that stabilizes and hence, increases the protein level of the oncogene c-myc in IEC²³. This sequence of events enhances IEC proliferation and reduces IEC apoptosis and therefore promotes IEC tumor growth in *Apc^{min/+}* mice.

The oncogene *c-myc* is a Wnt target gene^{33,34}. While β -catenin/TCF signaling induces *c-myc* transcriptionally, its expression levels are heavily regulated by ubiquitin-mediated proteasomal degradation^{35,36} which can be antagonized by pERK phosphorylation of c-myc^{23,24,25}. Our findings indicate that Myd88-dependent, ERK activation is essential to stabilize c-myc levels (Fig. 4), that the activation of ERK by a MyD88-independent ligand, EGF³⁷, increases c-myc levels and restores the Min phenotype in the *Apc^{min/+}/Myd88^{-/-}* mice (Fig. 5), and that treatment with a specific ERK inhibitor suppresses tumor development in both *Apc^{min/+}* and EGF-treated *Apc^{min/+}/Myd88^{-/-}* mice (Fig. 5 and Fig. 6). Collectively, these data indicate that 1) the loss of heterozygosity of *Apc* is insufficient to drive the Min phenotype in the *Apc^{min/+}* mouse, 2) that the synergy between c-myc transcription and post-translational modifications are required for tumor growth in this model, 3) activation of ERK is essential for IEC tumorigenesis in the *Apc^{min/+}* mouse and 4) that ERK functions as a major regulator of c-myc expression in the intestinal epithelium (Fig. 6H).

One mechanism that explains tumor suppression due to the inactivation of a single gene product is termed oncogene addiction. This phenomenon occurs when tumors require sustained activation of a single oncogene for their growth and survival, despite other oncogenic events⁹. Our data reveal that the IEC tumor growth in the *Apc^{min/+}* mice is due to pERK “addiction”. ERK addiction was shown recently to drive the survival of certain intestinal epithelial cell lines *in vitro*³⁸, although via a different pathway. Activation of ERK in this setting is most likely induced by a TLR-MyD88-dependent pathway (e.g., microflora, Fig. 3) and by a TLR-Myd88-independent pathway (e.g., growth factors) (Fig. 5). Consequently, the inhibition of ERK prevents tumorigenesis in *Apc^{min/+}* mice, most likely via the generation of an unstable c-myc protein (Fig. 5-6) leading to low c-myc levels in IEC (Fig. 3). Although the regulation of the ERK-c-myc pathway is sufficient for the inhibition of the Min phenotype under the steady state conditions, and its reversal upon EGF administration, in *Apc^{min/+}/Myd88^{-/-}* mice, we can't rule out other anti-apoptotic effects provoked by pERK³⁸ in IEC of these animals.

The dichotomy in tumor numbers between *Apc^{min/+}* and *Apc^{min/+}/Myd88^{-/-}* mice (Supp. Fig. 1), as well as the biochemical evidence presented above *in vitro* (Fig. 4) and *in vivo* (Fig. 5-6), highly suggest the inductive role of microflora-derived MyD88 signaling on IEC tumorigenesis in *Apc^{min/+}* mice. These observations reveal a new facet of oncogene-environment interactions, which might explain why a germline mutation in *Apc* results primarily in tumors originating from the intestinal epithelium (Fig. 6H) and not in other organs. Since pERK is a major player in the induction of the Min phenotype (Fig. 5-6), we propose that interventions aimed at inhibiting ERK activation in IEC (Fig. 6) may help suppress the induction of IEC neoplasia in humans with variant *Apc* genes.

Materials and Methods

Materials

The following antibodies were obtained from Cell Signaling Technology (Danvers, MA): anti-phospho ERK1/2, anti-ERK1/2, anti-c-myc, anti-PARP, anti- β -catenin, anti-PCNA and anti-MyD88. Anti-ubiquitin antibody was purchased from Santa Cruz Biotechnology (Santa Cruz, CA) and anti-phospho-c-myc (Ser62) antibody for IB and anti-c-myc antibody for immunohistochemistry from Abcam (Cambridge, MA). InSolution™ MG-132 was purchased from Calbiochem (San Diego, CA), the MEK1/2 inhibitor (U0126) from Promega (Madison, WI) and the MEK1/2 inhibitor, PD0325901, from Stemgent (San Diego, CA). Anakinra was purchased from Amgen (Kineret®, CA), recombinant mEGF from PeproTech, Inc. (Rocky Hill, NJ), the TLR2 ligand, Pam3Cys (P3C) from InvivoGen (San Diego, CA) and the Wnt3a from R&D system (Minneapolis, MN).

Mice

C57Bl/6J, *Apc^{min/+}* and *Il1r1^{-/-}* mice were purchased from The Jackson Laboratory (Bar Harbor, ME). *Myd88^{-/-}* mice were kindly provided by Dr. S. Akira (Osaka University, Japan), and were backcrossed 10 generations onto C57Bl/6, *Lps2* by Dr. B. Beutler (TSRI, San Diego, CA) and *Caspase1^{-/-}* mice by Dr. R. Flavell (Yale University, CT). All these

mice strain were crossed to *Apc^{min/+}* mice. All animal protocols received prior approval by the Institutional Review Board.

***In vivo* treatment with Anakinra**

Eight to 10 week-old mice *Apc^{min/+}* mice were injected i.p with 50 mg/kg of Anakinra, 5 times/week for ten weeks and analyzed when they reached 20 weeks of age.

***In vivo* treatment with EGF**

Eight to 10 week-old mice were injected i.p with EGF (2 µg/mouse), 3 times/week for 10 weeks and analyzed when they reached 20 weeks of age.

***In vivo* treatment with an ERK inhibitor**

PD0325901 was dissolved initially in DMSO (50 mg/ml) as a stock solution. The stock solution was then diluted fresh in water containing 0.05% (Hydroxypropyl)methylcellulose and 0.02% Tween 80. The formulation containing PD0325901 in 250 µl at the 25 mg/kg dose was administered by gavage three times a week to EGF-treated *Apc^{min/+}/Myd88^{-/-}* mice or five times a week to *Apc^{min/+}* mice, for the duration of each study. Controls mice were treated with vehicle (gavage).

Bone marrow (BM) chimeras were generated by reconstituting irradiated (9 Gy of γ -radiation) 6-10 week-old *Apc^{min/+}* and *Apc^{min/+}/Myd88^{-/-}* mice with BM cells (1.5×10^7 , i.v.) from sex-matched WT or *Myd88^{-/-}* donor mice. Chimerism was verified by qPCR of peripheral blood cells. Polyp counts were performed when mice reached 20 weeks of age.

BrdU staining was performed using a BrdU *in situ* staining kit (BD Biosciences, San Diego, CA). Mice were injected i.p. with 2 mg of BrdU solution. Intestinal tissue samples were fixed with formalin and embedded in paraffin. Immunostaining for labeled BrdU was performed according to the manufacturer's instruction. The enumeration of BrdU positioning was performed as described ³⁹.

TUNEL assay was performed on paraffinized intestinal tissues according to the manufacturer's instruction (BD Biosciences). Nuclei were stained with Hoechst 33258 (Invitrogen, Carlsbad, CA).

Isolation of intestinal epithelial cells, RT-PCR, Immunoblotting and immunoprecipitation were performed as previously described ¹⁹.

Cell Culture

The human IEC cell lines RKO and Caco-2 were cultured in DMEM supplemented with 4.0 mM glutamine, 10% fetal calf serum, 50 U/ml penicillin and 50 µg/ml streptomycin.

siRNA-mediated knockdown

Myd88 siRNA or *c-myc* siRNA from Santa Cruz Biotechnology (Santa Cruz, CA). Briefly, siRNA (40 µM) in 50 µl of Opti-MEM (Invitrogen) was mixed with 5 µl of Dharmafect 4 (Dharmacon, Chicago, IL) in 50 µl of Opti-MEM. After 30 min incubation at RT, the

transfection mixture was combined with 1×10^6 cells in culture medium. Non-targeting siRNA #2 (luciferase targeting siRNA) from Dharmacon was used as a control.

Histology and Immunohistochemistry (IHC)

DSI and colon were fixed in 10% formalin, paraffin embedded, and sectioned at 3 to 6 μm for H&E staining or immunostaining. The tissue sections were incubated with rabbit anti-c-myc ab (1:50), rabbit anti-pERK ab, or with control ab, overnight at 4°C. After washing with PBS, sections were incubated in HRP-conjugated secondary antibody for an hour and the staining was visualized with AEC peroxidase substrate kit (Vector Laboratories, Inc., Burlingame, CA), with hematoxylin nuclear counterstaining.

Blood hemoglobin was measured on a MS9 Blood Analyzer (Melet Schloesing Laboratories, El Cajon, CA) according to the manufacturer's instructions.

Statistical analysis was performed by Student's *t* test for paired samples or two-way ANOVA for multiple comparisons and by log-rank analysis for survival curves. Data are presented as means \pm s.d.

Supplementary Material

Refer to Web version on PubMed Central for supplementary material.

Acknowledgments

The authors thank Patty Charos for animal breeding and Steve Shenouda for tissue processing.

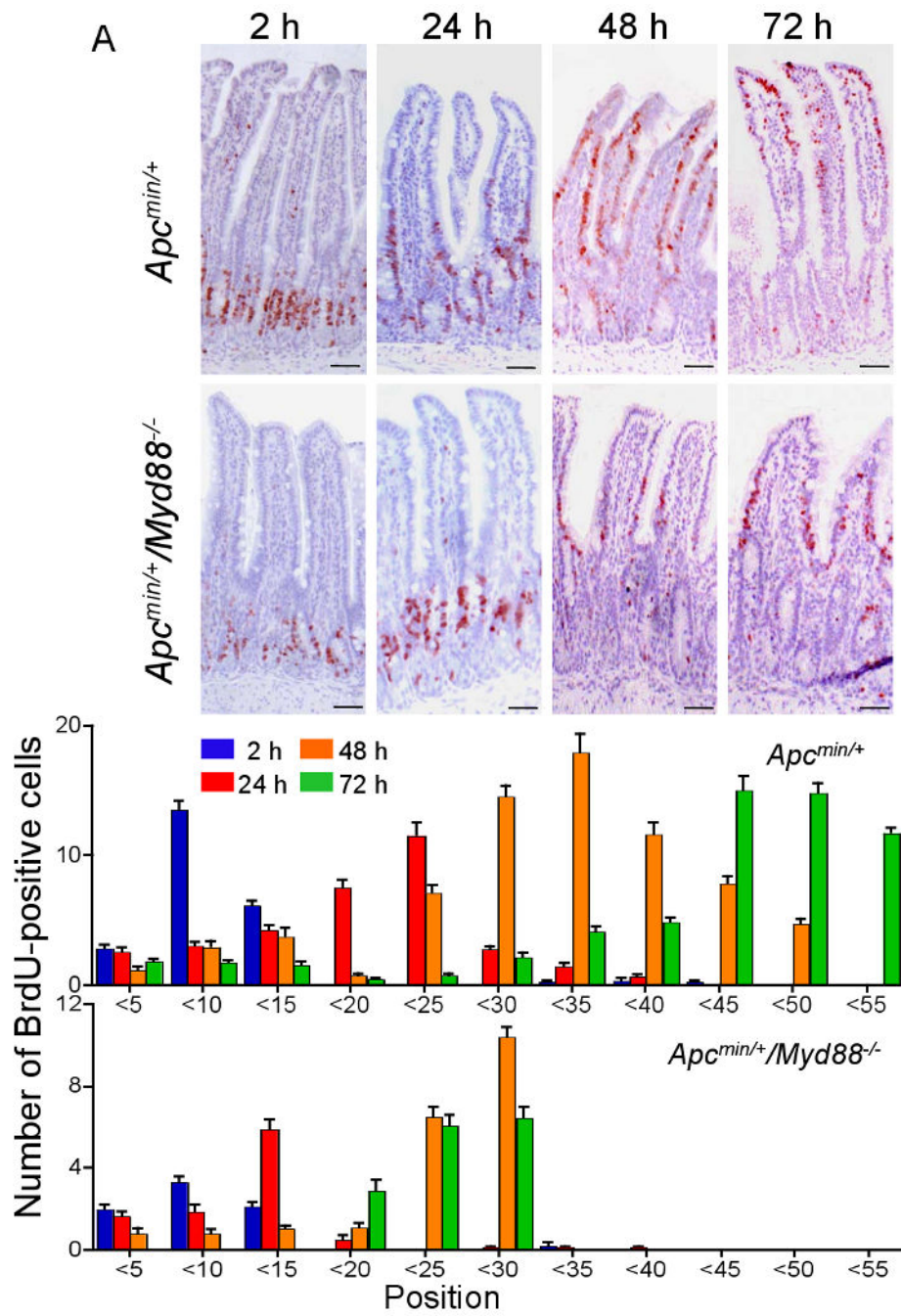
This work was supported by NIH grants AI068685, CA133702, DK35108 and DK080506.

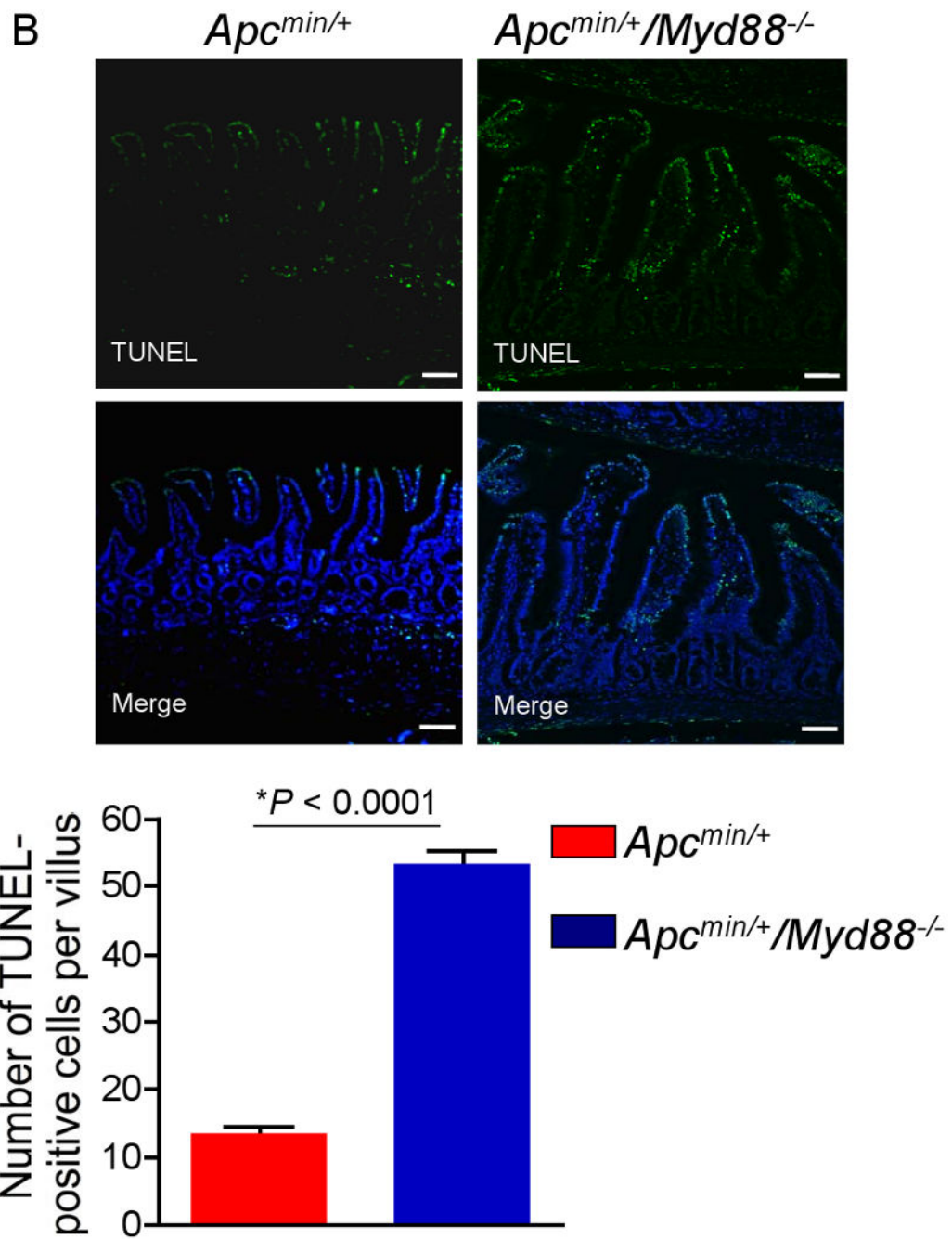
References

1. Michelsen KS, Arditi M. Toll-like receptors and innate immunity in gut homeostasis and pathology. *Curr Opin Hematol.* 2007; 14:48–54. [PubMed: 17133100]
2. Sanderson IR, Walker WA. TLRs in the Gut I. The role of TLRs/Nods in intestinal development and homeostasis. *Am J Physiol Gastrointest Liver Physiol.* 2007; 292:G6–10. [PubMed: 16844677]
3. de Visser KE, Eichten A, Coussens LM. Paradoxical roles of the immune system during cancer development. *Nat Rev Cancer.* 2006; 6:24–37. [PubMed: 16397525]
4. Karin M. Nuclear factor-kappaB in cancer development and progression. *Nature.* 2006; 441:431–436. [PubMed: 16724054]
5. Lin WW, Karin M. A cytokine-mediated link between innate immunity, inflammation, and cancer. *J Clin Invest.* 2007; 117:1175–1183. [PubMed: 17476347]
6. Rakoff-Nahoum S, Medzhitov R. Regulation of spontaneous intestinal tumorigenesis through the adaptor protein Myd88. *Science.* 2007; 317:124–127. [PubMed: 17615359]
7. Oshima M, et al. Loss of Apc heterozygosity and abnormal tissue building in nascent intestinal polyps in mice carrying a truncated Apc gene. *Proc Natl Acad Sci U S A.* 1995; 92:4482–4486. [PubMed: 7753829]
8. Moser AR, Pitot HC, Dove WF. A dominant mutation that predisposes to multiple intestinal neoplasia in the mouse. *Science.* 1990; 247:322–324. [PubMed: 2296722]
9. Weinstein IB. Cancer. Addiction to oncogenes--the Achilles heel of cancer. *Science.* 2002; 297:63–64. [PubMed: 12098689]
10. Hurlin PJ, Huang J. The MAX-interacting transcription factor network. *Semin Cancer Biol.* 2006; 16:265–274. [PubMed: 16908182]

11. Wilkins JA, Sansom OJ. C-Myc is a critical mediator of the phenotypes of Apc loss in the intestine. *Cancer Res.* 2008; 68:4963–4966. [PubMed: 18593890]
12. Sansom OJ, et al. Myc deletion rescues Apc deficiency in the small intestine. *Nature.* 2007; 446:676–679. [PubMed: 17377531]
13. Yekkala K, Baudino TA. Inhibition of intestinal polyposis with reduced angiogenesis in Apcmin/+mice due to decreases in c-Myc expression. *Mol Cancer Res.* 2007; 5:1296–1303. [PubMed: 18171987]
14. Ignatenko NA, et al. Role of c-Myc in intestinal tumorigenesis of the Apcmin/+mouse. *Cancer Biol Ther.* 2006; 5:1658–1664. [PubMed: 17106247]
15. Beutler B, et al. Genetic analysis of host resistance: Toll-like receptor signaling and immunity at large. *Annu Rev Immunol.* 2006; 24:353–389. [PubMed: 16551253]
16. Boulares AH, et al. Role of poly(ADP-ribose) polymerase (PARP) cleavage in apoptosis. Caspase 3-resistant PARP mutant increases rates of apoptosis in transfected cells. *J Biol Chem.* 1999; 274:22932–22940. [PubMed: 10438458]
17. Kelsall BL, Rescigno M. Mucosal dendritic cells in immunity and inflammation. *Nat Immunol.* 2004; 5:1091–1095. [PubMed: 15496943]
18. Cario E, et al. Commensal-associated molecular patterns induce selective toll-like receptor-traffic from apical membrane to cytoplasmic compartments in polarized intestinal epithelium. *Am J Pathol.* 2002; 160:165–173. [PubMed: 11786410]
19. Lee J, et al. Maintenance of colonic homeostasis by distinctive apical TLR9 signalling in intestinal epithelial cells. *Nat Cell Biol.* 2006; 8:1327–1336. [PubMed: 17128265]
20. Cho HJ, et al. IFN-alpha beta promote priming of antigen-specific CD8+ and CD4+ T lymphocytes by immunostimulatory DNA-based vaccines. *J Immunol.* 2002; 168:4907–4913. [PubMed: 11994440]
21. Apte RN, et al. The involvement of IL-1 in tumorigenesis, tumor invasiveness, metastasis and tumor-host interactions. *Cancer Metastasis Rev.* 2006; 25:387–408. [PubMed: 17043764]
22. Pedersen G, Andresen L, Matthiessen MW, Rask-Madsen J, Brynskov J. Expression of Toll-like receptor 9 and response to bacterial CpG oligodeoxynucleotides in human intestinal epithelium. *Clin Exp Immunol.* 2005; 141:298–306. [PubMed: 15996194]
23. Sears R, et al. Multiple Ras-dependent phosphorylation pathways regulate Myc protein stability. *Genes Dev.* 2000; 14:2501–2514. [PubMed: 11018017]
24. Sears RC. The life cycle of C-myc: from synthesis to degradation. *Cell Cycle.* 2004; 3:1133–1137. [PubMed: 15467447]
25. Vervoorts J, Luscher-Firzlaff J, Luscher B. The ins and outs of MYC regulation by posttranslational mechanisms. *J Biol Chem.* 2006; 281:34725–34729. [PubMed: 16987807]
26. Chang WC, et al. Sulindac sulfone is most effective in modulating beta-catenin-mediated transcription in cells with mutant APC. *Ann N Y Acad Sci.* 2005; 1059:41–55. [PubMed: 16382042]
27. Barrett SD, et al. The discovery of the benzhydroxamate MEK inhibitors CI-1040 and PD 0325901. *Bioorg Med Chem Lett.* 2008; 18:6501–6504. [PubMed: 18952427]
28. Seo TC, Spallholz JE, Yun HK, Kim SW. Selenium-enriched garlic and cabbage as a dietary selenium source for broilers. *J Med Food.* 2008; 11:687–692. [PubMed: 19053861]
29. Coussens LM, Werb Z. Inflammation and cancer. *Nature.* 2002; 420:860–867. [PubMed: 12490959]
30. Shacter E, Weitzman SA. Chronic inflammation and cancer. *Oncology (Williston Park).* 2002; 16:217–26. 229. discussion 230-2. [PubMed: 11866137]
31. Fox JG, Wang TC. Inflammation, atrophy, and gastric cancer. *J Clin Invest.* 2007; 117:60–69. [PubMed: 17200707]
32. Pikarsky E, et al. NF-kappaB functions as a tumour promoter in inflammation-associated cancer. *Nature.* 2004; 431:461–466. [PubMed: 15329734]
33. He TC, et al. Identification of c-MYC as a target of the APC pathway. *Science.* 1998; 281:1509–1512. [PubMed: 9727977]

34. Dang CV, et al. The c-Myc target gene network. *Semin Cancer Biol.* 2006; 16:253–264. [PubMed: 16904903]
35. Hann SR. Role of post-translational modifications in regulating c-Myc proteolysis, transcriptional activity and biological function. *Semin Cancer Biol.* 2006; 16:288–302. [PubMed: 16938463]
36. Gregory MA, Hann SR. c-Myc proteolysis by the ubiquitin-proteasome pathway: stabilization of c-Myc in Burkitt's lymphoma cells. *Mol Cell Biol.* 2000; 20:2423–2435. [PubMed: 10713166]
37. Dakour J, Li H, Chen H, Morrish DW. EGF promotes development of a differentiated trophoblast phenotype having c-myc and junB proto-oncogene activation. *Placenta.* 1999; 20:119–126. [PubMed: 9950153]
38. Wickenden JA, et al. Colorectal cancer cells with the BRAF(V600E) mutation are addicted to the ERK1/2 pathway for growth factor-independent survival and repression of BIM. *Oncogene.* 2008; 27:7150–7161. [PubMed: 18806830]
39. Sansom OJ, et al. Loss of Apc in vivo immediately perturbs Wnt signaling, differentiation, and migration. *Genes Dev.* 2004; 18:1385–1390. [PubMed: 15198980]
40. Dove WF, et al. Intestinal neoplasia in the ApcMin mouse: independence from the microbial and natural killer (beige locus) status. *Cancer Res.* 1997; 57:812–814. [PubMed: 9041176]





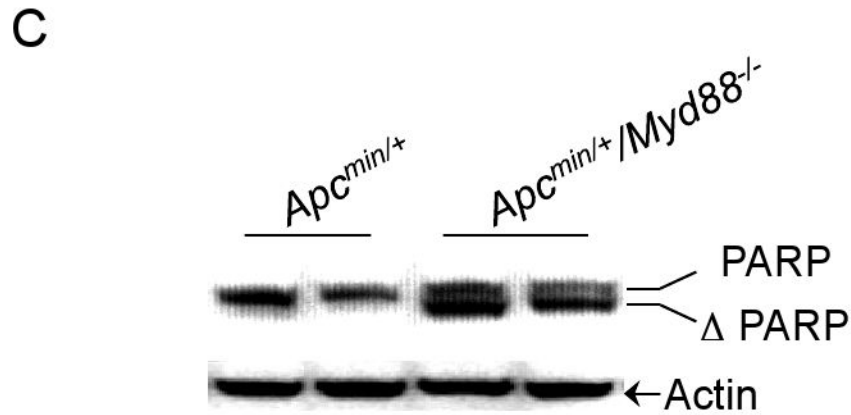
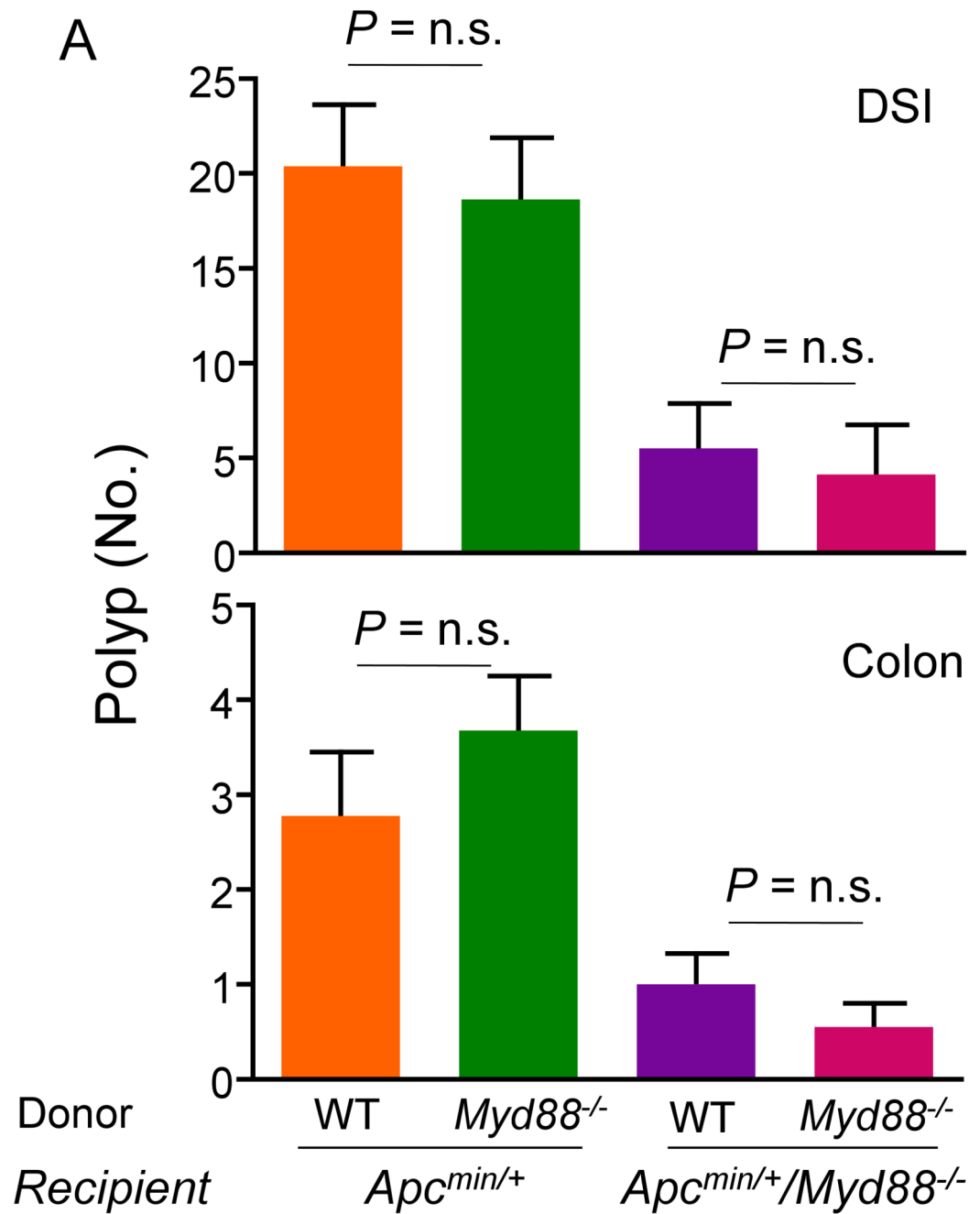


Figure 1. Genetic disruption of *Myd88* in *Apc^{min/+}* mice suppresses proliferation and enhances apoptosis of IEC

A. IHC and BrdU incorporation in IEC (DSI) after i.p. BrdU injection (scale bars - 20 μ m, magnification \times 200). BrdU-positive cells, per time point, were enumerated for each indicated position in a crypt (10 crypt-villi units/time point), position 0 being the base of the crypt³⁹. **B.** Apoptotic IEC (DSI) were determined by TUNEL assay (scale bars - 40 μ m, magnification \times 100). **C.** Cleaved product of poly(ADP-ribose) polymerase (PARP) in IEC (DSI) harvested from the indicated mice ($n=2$ /group).



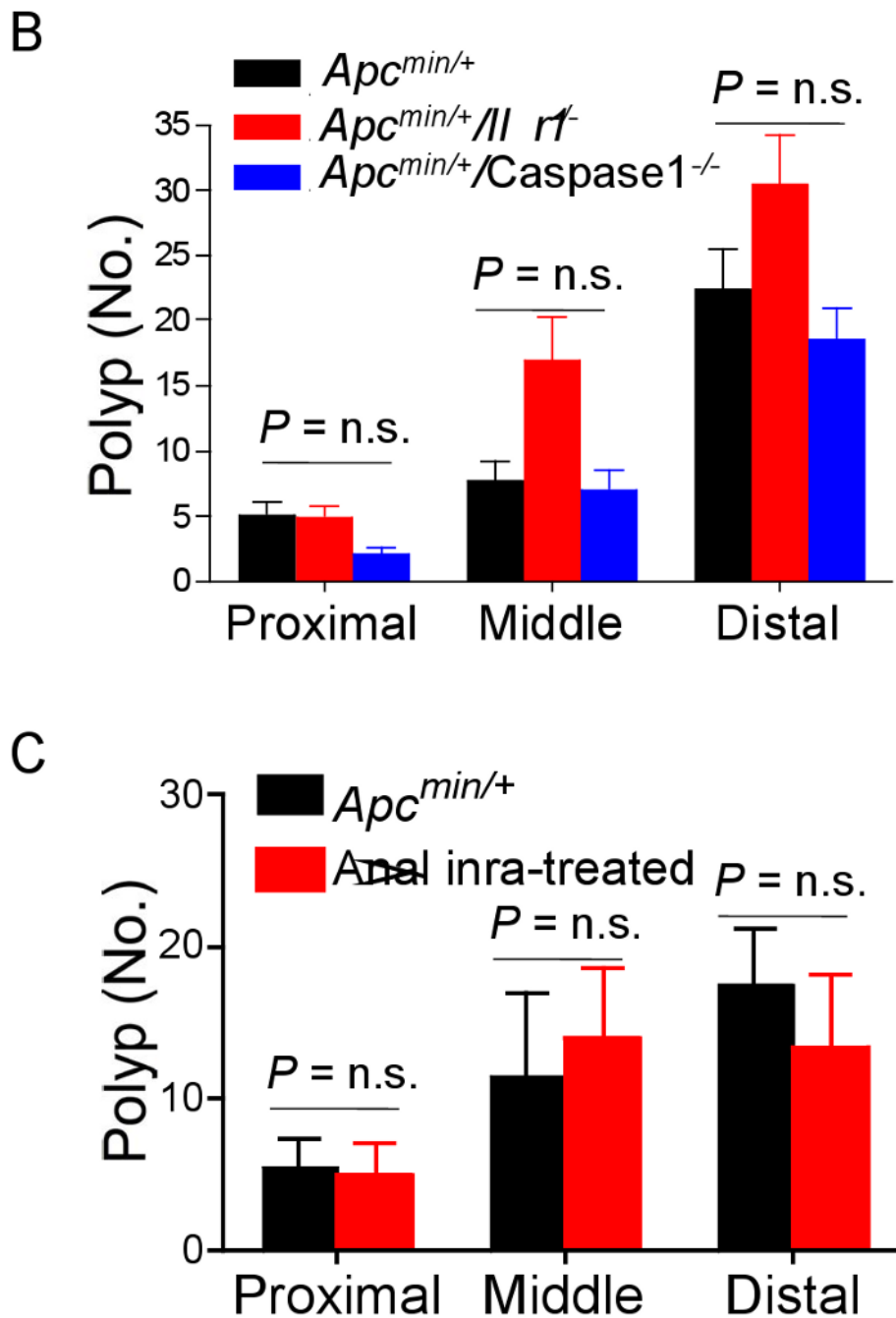


Figure 2. Myd88 signaling in hematopoietic cells is not required for tumorigenesis in *Apc*^{min/+} mice

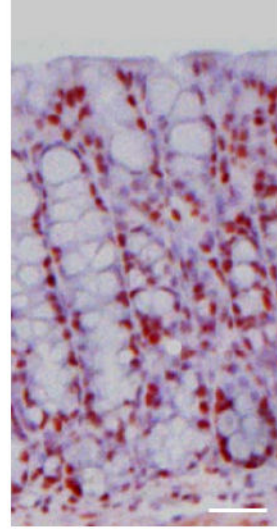
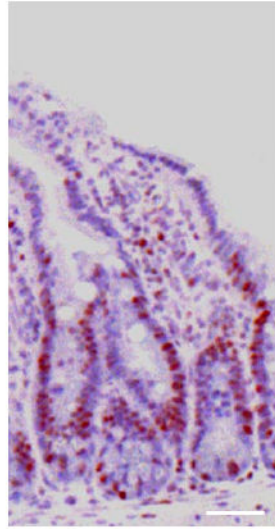
A. Polyp count in BM chimeras in the DSI and colon ($P=n.s.$, $n=7-9$ mice/group). **B.** Polyp count in the small intestine in *Apc*^{min/+}/*Irr1*^{-/-} and *Apc*^{min/+}/*Caspase1*^{-/-} mice at 20 weeks of age ($n=7$ /group). **C.** Polyp count in Anakinra-treated *Apc*^{min/+} mice (DSI) ($P=n.s.$, $n=7$ /group).

A

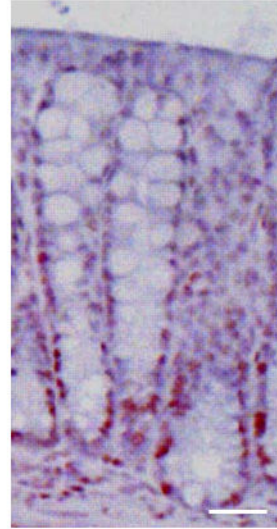
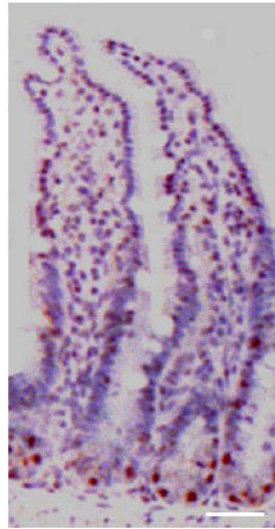
DSI

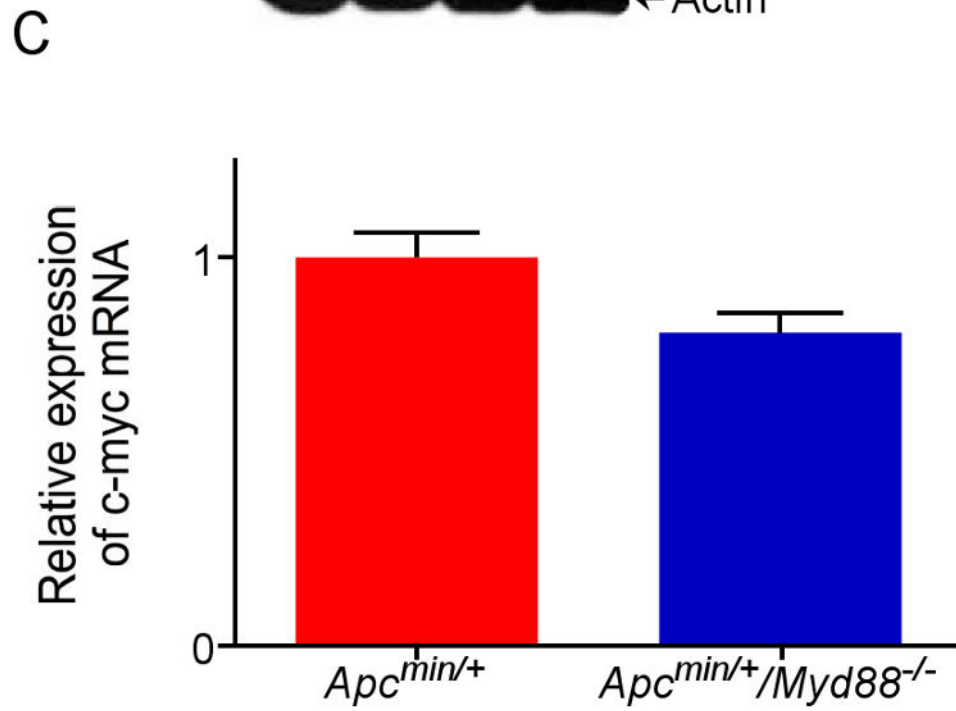
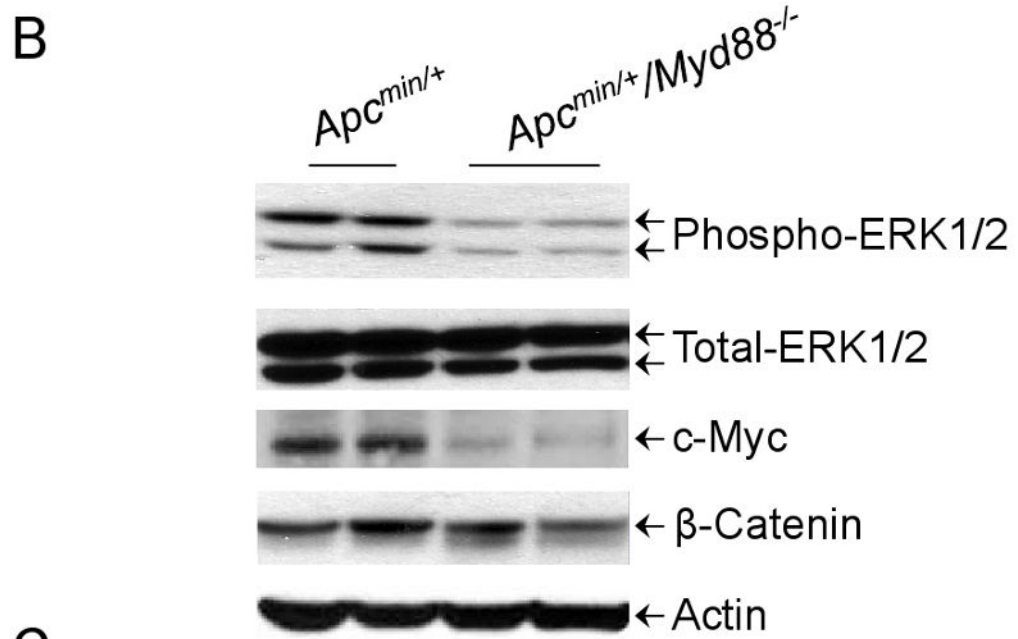
Colon

Apc^{min/+}



Apc^{min/+}/Myd88^{-/-}





D

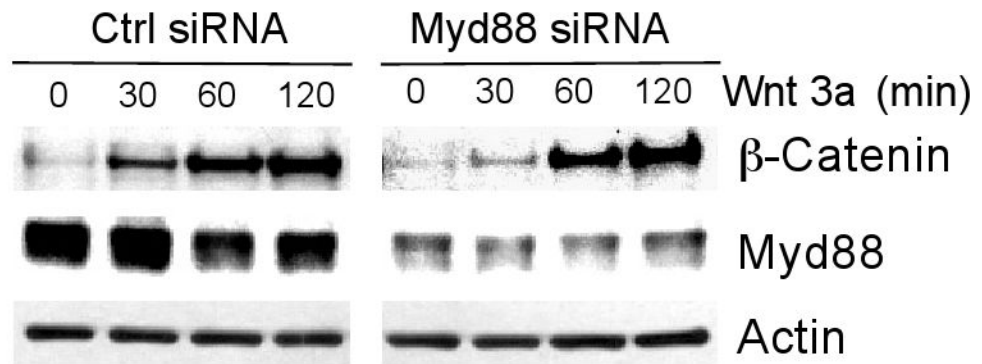
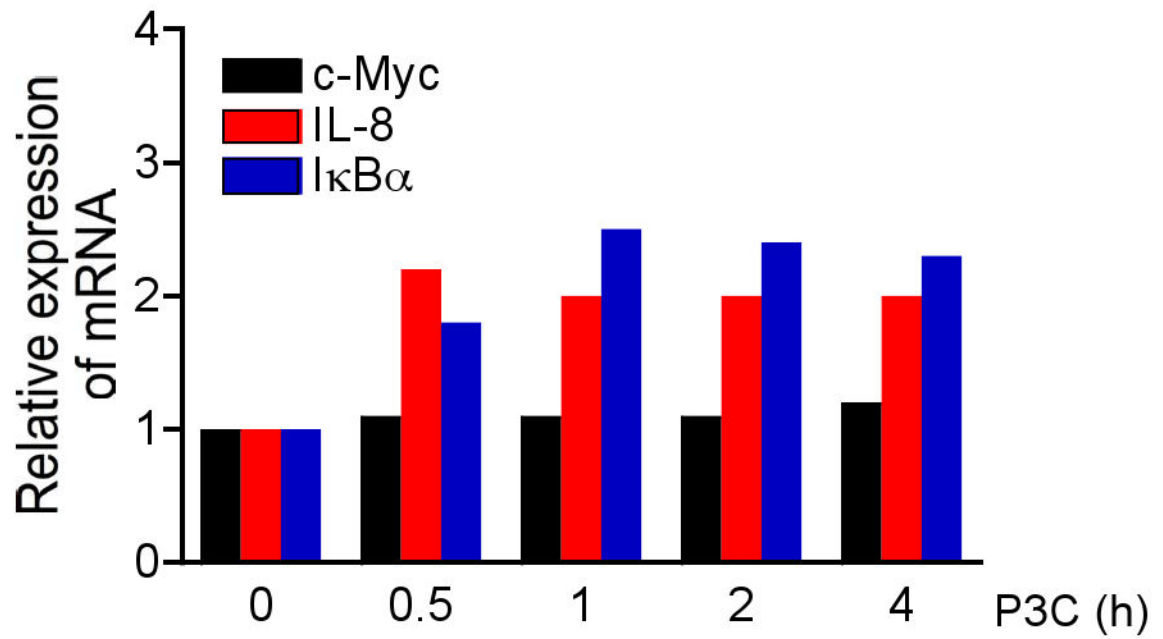
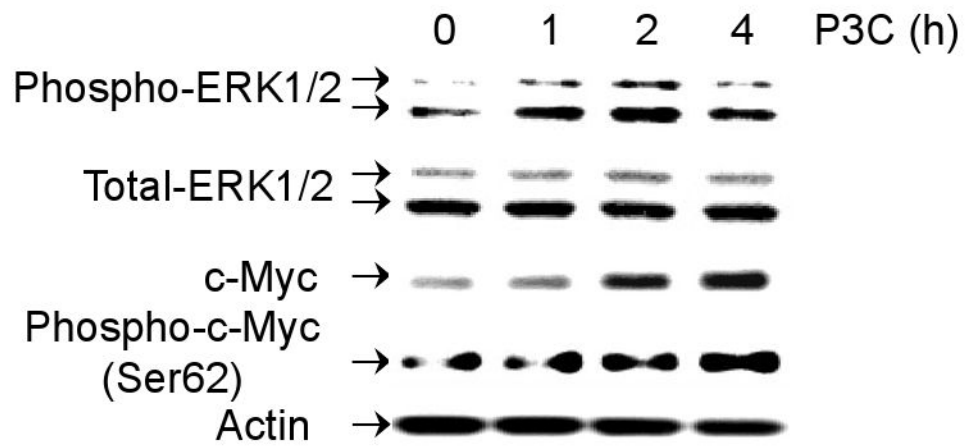
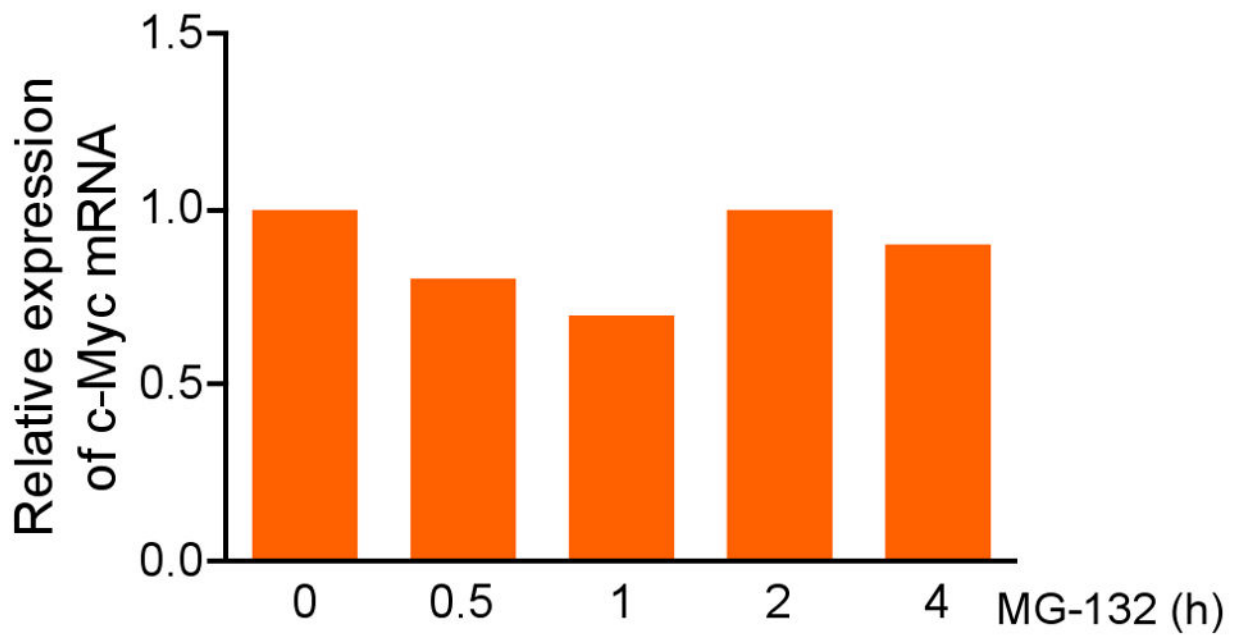
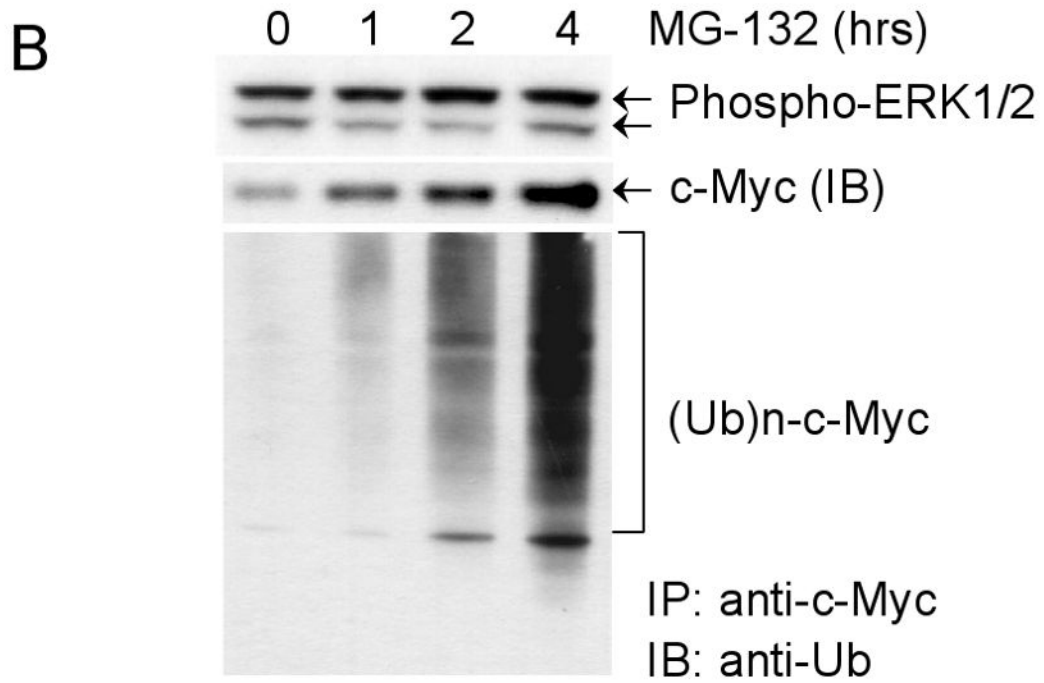


Figure 3. MyD88 regulates c-myc expression levels

A. IHC analysis of c-myc protein in IEC from the DSI and colon from 20-week old mice (scale bars, 10 μ m, magnification \times 200). **B.** IB analysis of the indicated proteins in IEC (DSI) of 20-weeks mice ($n=2$). **C.** Transcript levels of *c-myc* in IEC (DSI) ($P=n.s$, $n=3$ /group). **D.** RKO cells transfected with either control or *Myd88* siRNA, were stimulated with Wnt3a (100ng/ml) and subjected to IB analysis.

A





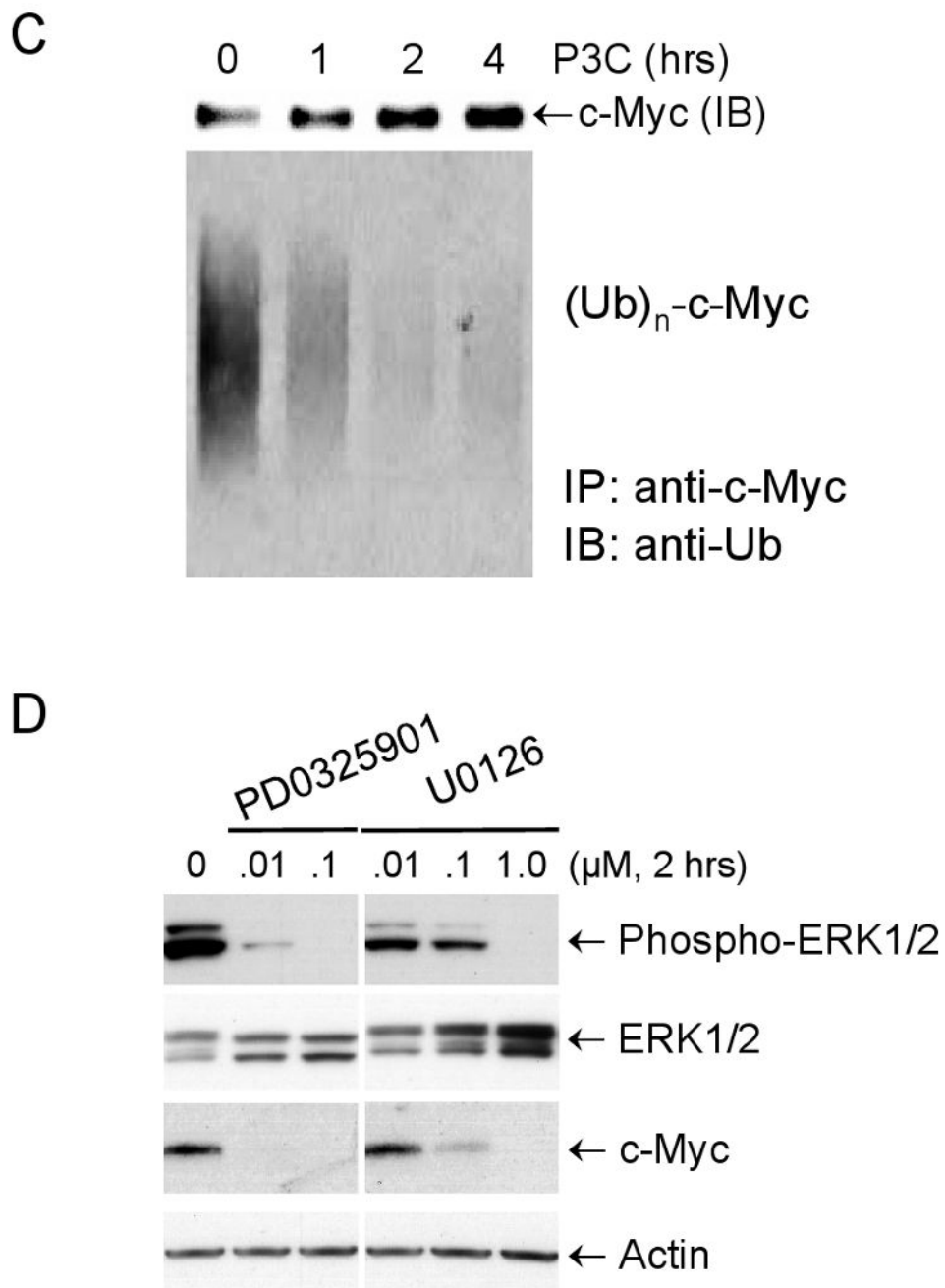
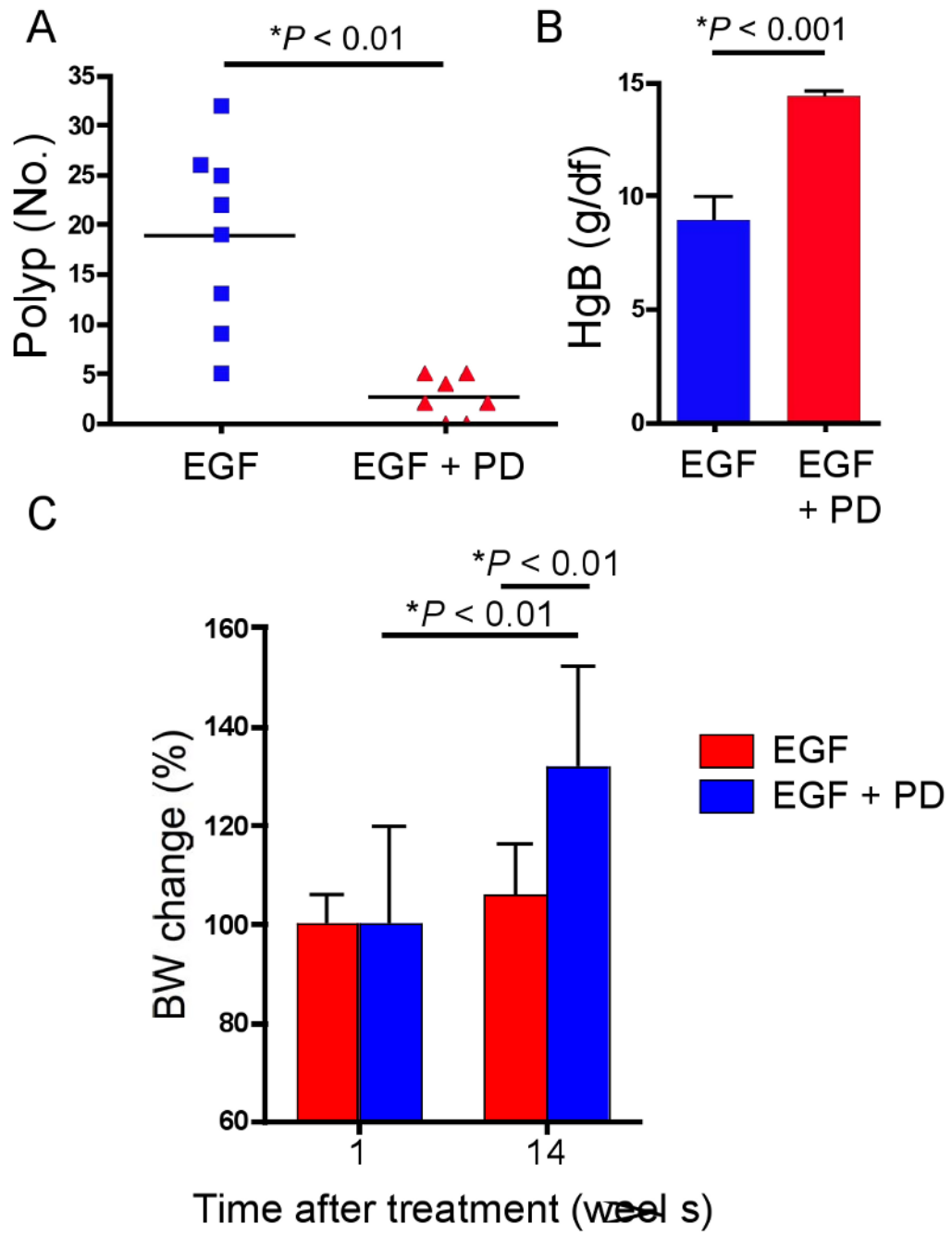


Figure 4. TLR signaling via MyD88 stabilizes c-myc protein in IEC through activation of ERK
A. Upper panel: RKO cells were stimulated with P3C (2 μg/ml), lysed and analyzed by IB. **Lower panel:** Transcript levels after TLR2 stimulation (qPCR). **B.** Protein levels (IB) (**Upper panel**) and transcript level (qPCR) (**Lower panel**) in MG-132 treated (10 μM) RKO cells. C-myc was immunoprecipitated followed by IB with anti-ubiquitin (Ub) ab. **C.** RKO cells were treated with P3C (2 μg/ml) and ubiquitinated c-myc level was measured by IP followed by IB. **D.** Phospho-ERK and c-myc levels (IB) in U0126- or PD0325901-treated RKO cells.



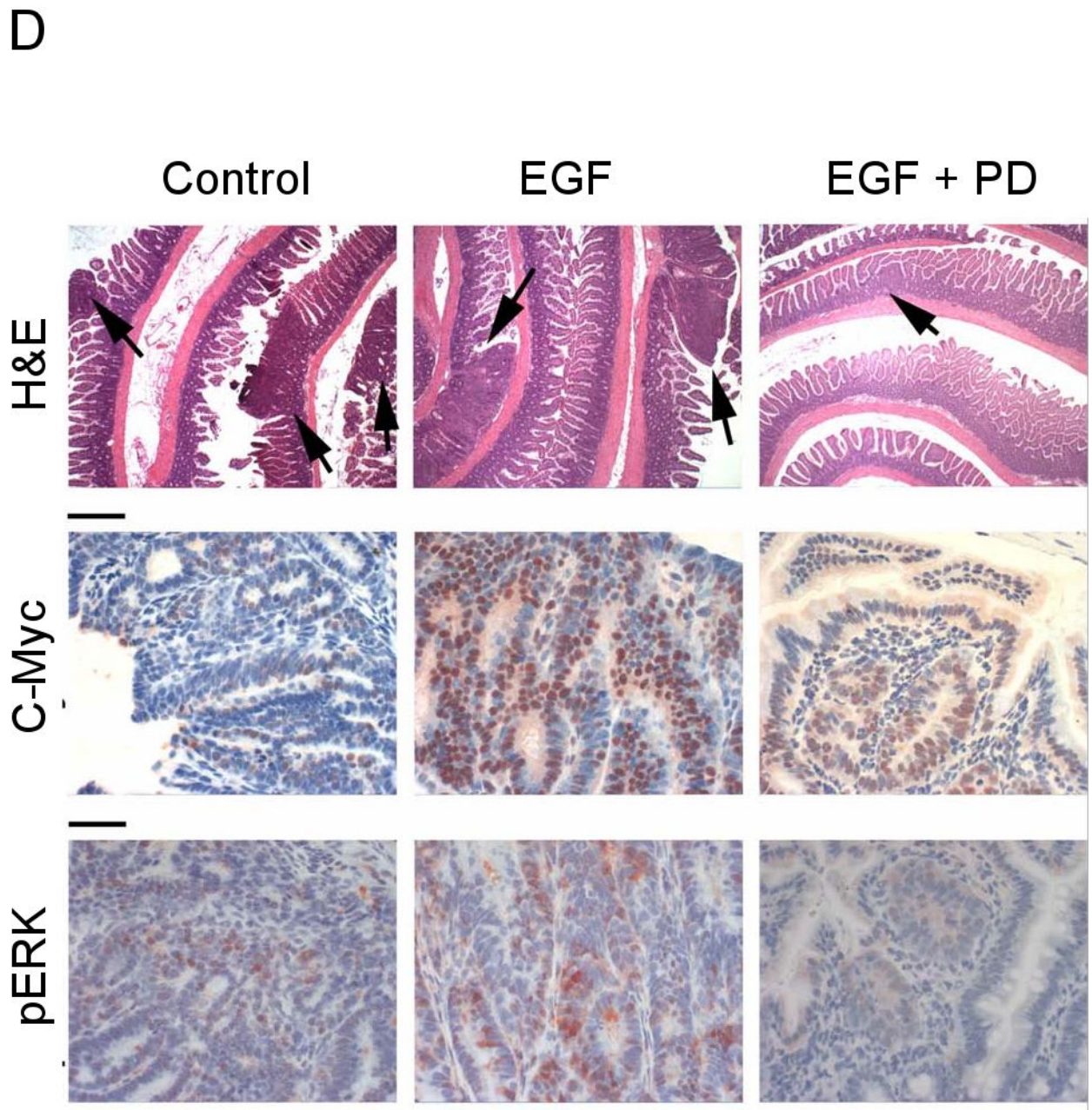
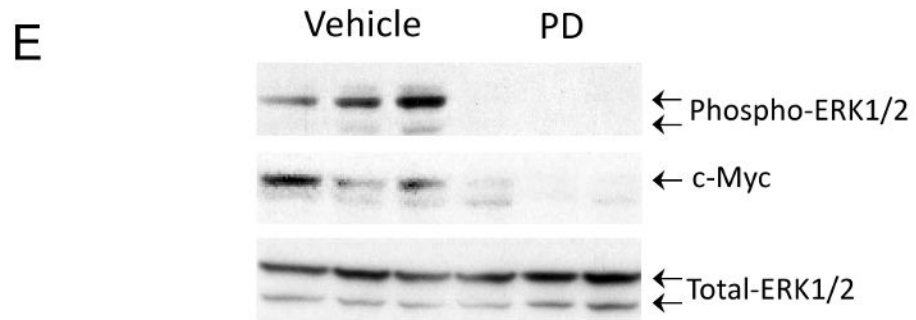
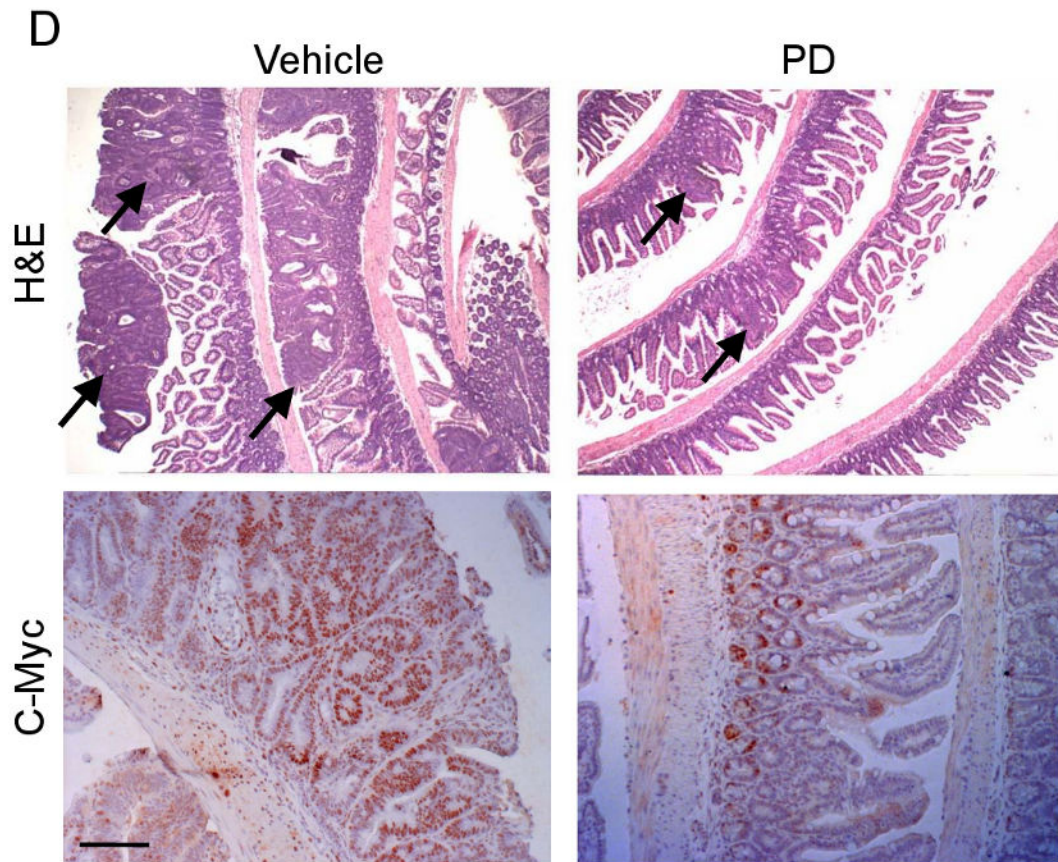
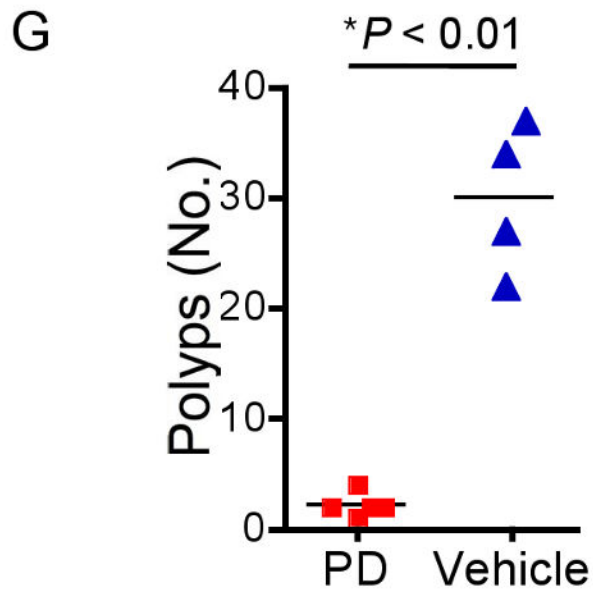
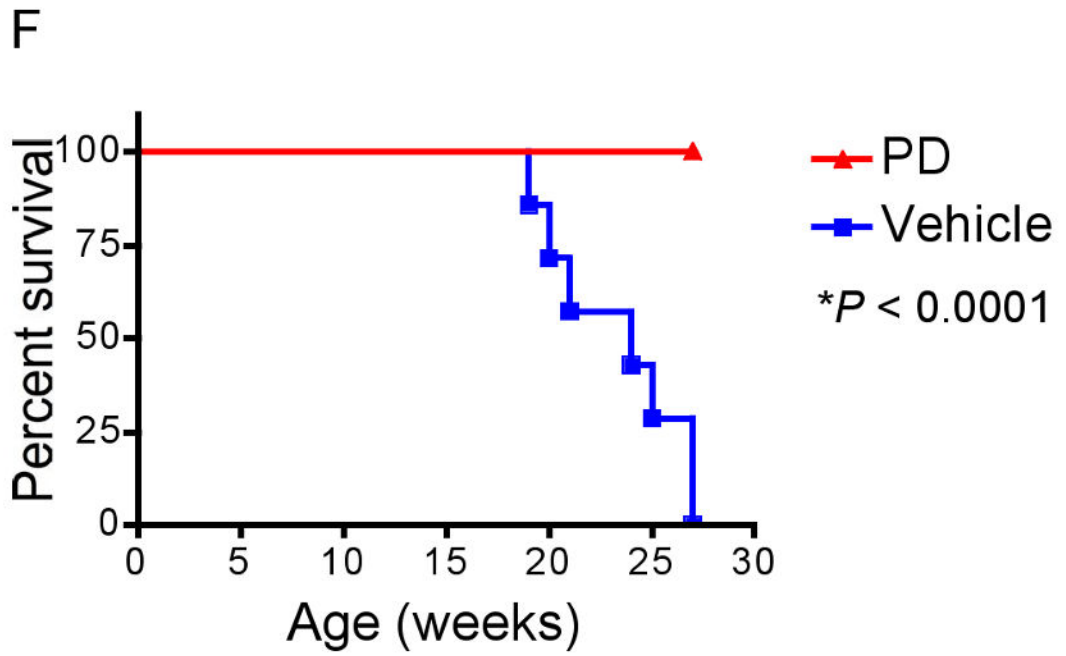


Figure 5. Activation of ERK restores the Min phenotype in *Apc^{min/+}/Myd88^{-/-}* mice
A. PD reduces the number of polyps in EGF-treated *Apc^{min/+}/Myd88^{-/-}* mice (DSI) ($n=8/$ group). **B.** Blood hemoglobin levels and **(C)** body weight of these mice. **D. Top panel:** H&E of DSI in control, EGF-treated, and EGF + PD-treated mice. The arrows indicate intestinal polyps. **Middle panel:** C-myc expression in IEC. **Bottom panel:** Phospho-ERK levels in IEC of these mice.





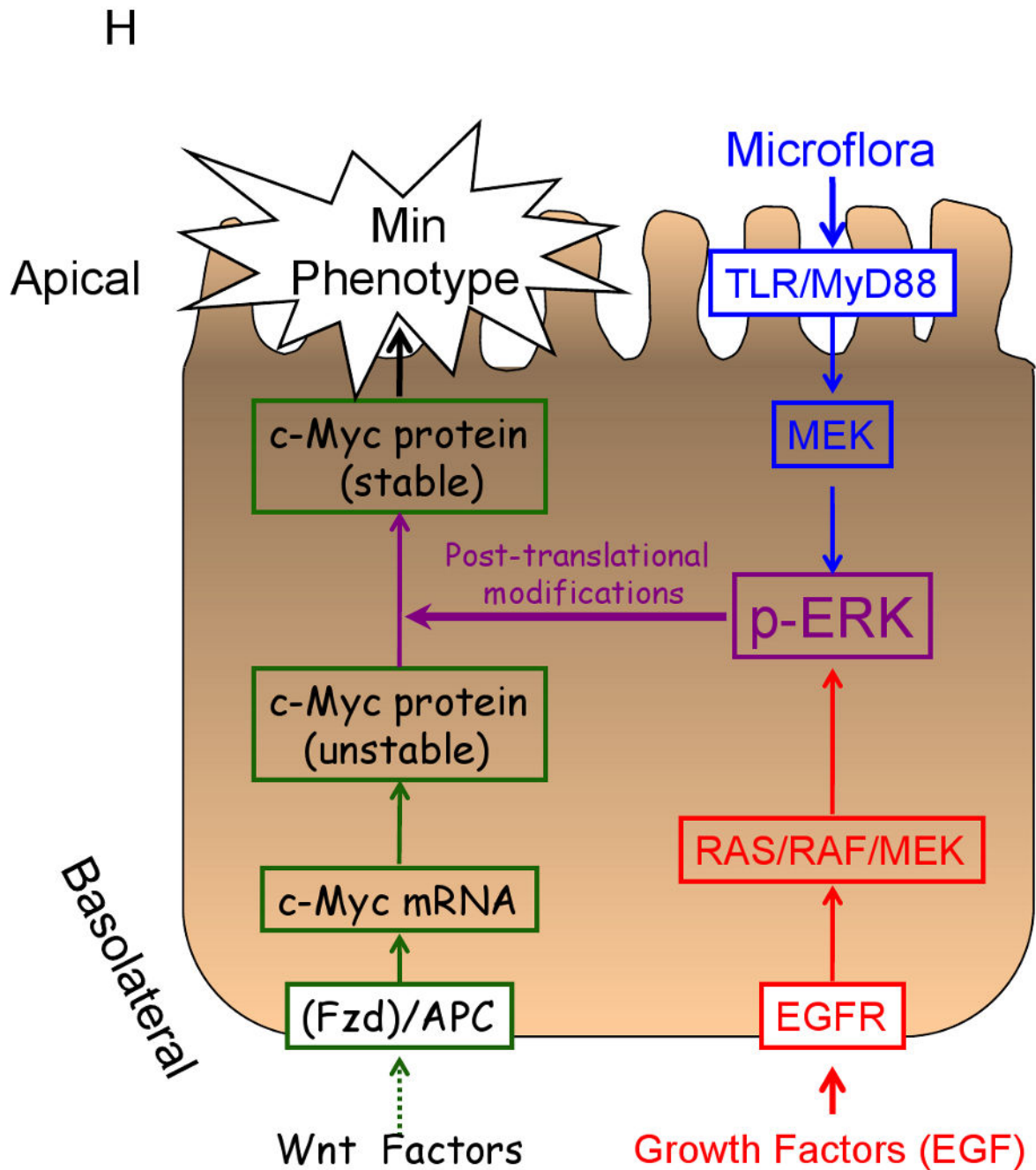


Figure 6. Activation of ERK is essential for the Min phenotype in $Apc^{min/+}$ mice

A. Polyp count, **B** hemoglobin level, and **C** body weight in PD-treated $Apc^{min/+}$ mice ($n=6$ for vehicle, $n=9$ for PD group). **D. Upper panel:** H&E of DSI in control and PD-treated $Apc^{min/+}$ mice. Arrows indicate intestinal polyps. **Lower panel:** C-myc expression in IEC. **E.** IB analysis of c-myc and pERK levels in IEC (DSI) of these mice. **F.** Survival in PD-treated or vehicle-treated $Apc^{min/+}$ mice for 17 weeks ($n=8$). **G.** The PD-treated $Apc^{min/+}$ mice mentioned in **F** were split to PD- and vehicle-treated groups ($n=4$ /group). Polyp count (DSI) was performed 15 weeks later. **H.** The microflora induces tumorigenesis in $Apc^{min/+}$

mice by triggering TLR-ERK pathway in IEC. This stabilizes c-myc and inhibits its proteasomal degradation. Increased c-myc levels induce the Min phenotype. Additional signals such as growth factors, utilize the MEK-ERK pathway and similarly to TLR ligands, can enhance c-myc levels. Of note, sterile food and water still contain TLR ligands (e.g., LPS) that are capable of stimulating IEC. This mechanism may account for the Min phenotype observed in *Apc^{min/+}* mice housed under germ-free conditions⁴⁰.

Author Manuscript

Author Manuscript

Author Manuscript

Author Manuscript